Density Peaking in T-10 L-mode Plasmas with ECRH

N.A. Kirneva[1)], I.V. Gubarev[1,2)], E.P. Gorbunov, D.A. Kislov[1)] , E.V. Trukhina[1)]

[1)] *RRC"Kurchatov Institute", Moscow, Russia*

[2)] *Moscow Engineering and Physics Institute, Moscow, Russia*

Flat density profile has been previously predicted for ITER [1]. However recent experiments on different tokamaks over the world have demonstrated increase of the density peaking factor $p_n=n_e(0)/<n_e>$ with collisionality decrease [2,3,4]. This has led to the conclusion that sufficiently more peaked density profile (with the peaking factor $p_n\cong 1.4\text{-}1.6$) could be expected in ITER H-mode discharges [2,3]. L-mode plasmas has demonstrated different dependence of density peaking factor on collisionality: p_n has been observed independent on collisionality in L-mode in JET and TCV [2], increase of density gradient with collisionality has been observed in FTU [5].

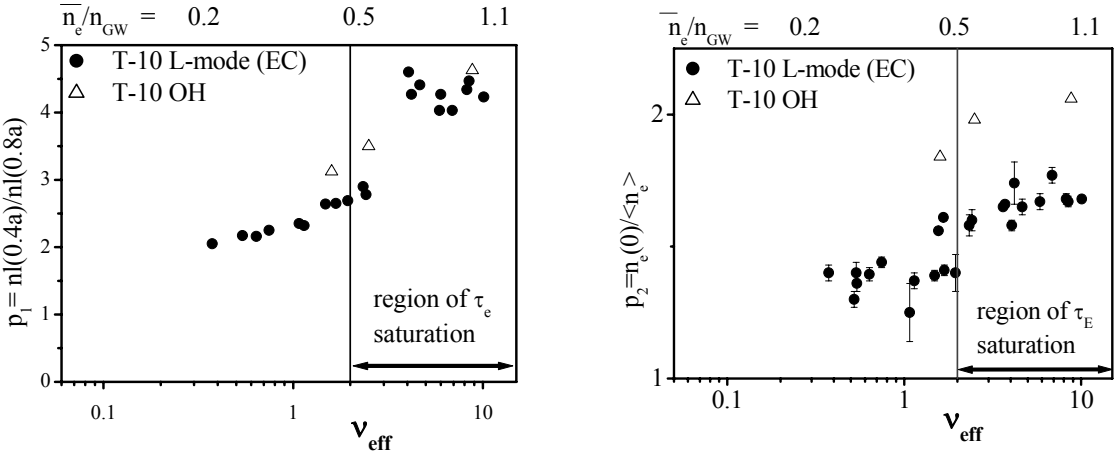

Fig. 1 Collisionality dependence of the density peaking factor in T-10 in OH regime (triangles) and in L-mode with ECRH (circles). P_{ECRH}=0.92 MW. In all discharges I_p=210 kA, q_L=3.5. Correspondence between Greenwald fraction and collisionality is given for ECRH case.

Experimental investigation of density profile behavior has been done in T-10 ECR heated plasmas (L-mode) in a wide range of plasma densities, $\bar{n}_e / n_{Gw} = 0.2 \div 1.1$. It has been shown that the density gradient increases with the density growth in T-10 ohmically heated plasmas and in L-mode with ECRH (on-axis heating, P_{ab}=0.92 MW) [6]. This grad(n_e) increase means the increase of the density peaking factor with collisionality (Fig.1). Density peaking factor, p_n, is characterized on Fig. 1 in two different ways: 1) p_1 is a ratio of signals from central (nl(0.4a)) and periphery (at Low Field Side, nl(0.8a)) chords of interferometer (Fig. 1,a) and 2) p_2 is a ratio of central plasma density, $n_e(0)$, to the volume average density value, $<n_e>$ (Fig. 1,b). Density profiles were reconstructed from 16-channels interferometer measurements. Note that the first definition of p_n allows us to exclude the region affected by

sawtooth oscillations (r<0.4a) and to decrease the error-bars appearing due to the solution of the inversion problem. Following the Ref. [4] collisionality value has been defined as $\nu_{eff} = 0.1 \cdot R \cdot z_{eff} \cdot n_e / T_e^2$. Here electron density, n_e, temperature, T_e, and the value of effective charge, z_{eff}, have been taken at the middle radius (r/a=0.5). As it seen from Fig. 1 density peaking increases with collisionality increase in T-10 experiments. Two regions can be marked in the dependence of density profile shape on collisionality. 1) The low collisionality region, $\nu_{eff} \leq 2$. Here the density peaking factor is relatively low: the p_1 value is increasing from 2.0 to 2.8, p_2=1.35±0.1 in L-mode plasmas. 2) High collisionality region, $\nu_{eff} > 2$. Here the peaking factor increases in comparison with the previous case and reaches p_1=4.3±0.3 and p_2=1.65±0.1 in L-mode. (In OH plasmas the picture is the similar, but peaking factor is higher in both collisionality regions that reflects so-called density pump-out effect.) Transition from low to high density peaking factor corresponds to the transition from linear $\tau_E(\bar{n}_e)$ dependence to the saturation of $\tau_E(\bar{n}_e)$ discussed in [6].

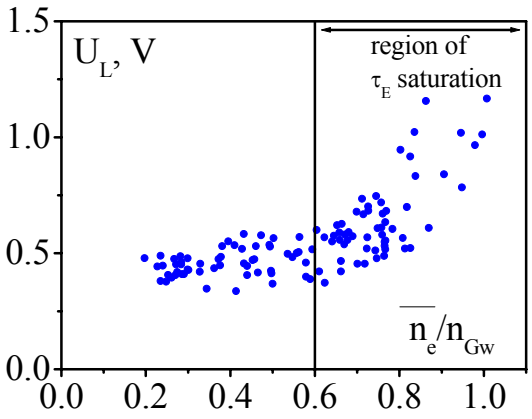

Fig. 2 Changes of loop voltage with density increase.

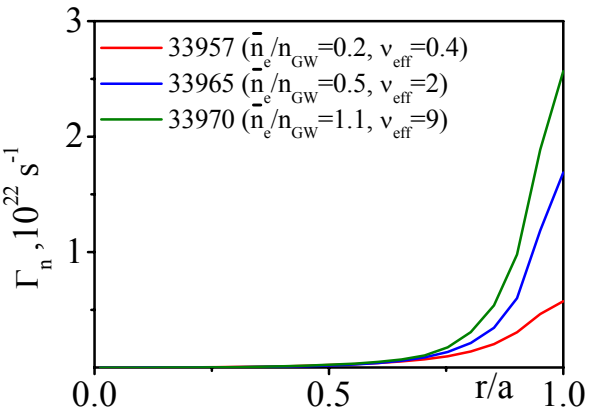

Fig. 3 Calculated neutral particle flux.

Increase of density peaking with collisionality in T-10 correlates with the increase of the loop voltage, U_L, i.e. $E_{||}$ (Fig. 2). Therefore the increase of the Ware pinch [7] can be proposed as a possible explanation of density profile behavior. Modeling has been done with the ASTRA transport code [8] to analyze the Ware pinch effect. Particle diffusivity has been chosen as $D_e = 0.5\chi_e$ and two models for particle pinch have been analyzed: $V_p^{(1)} = 1.5 V_{Ware}$ and $V_p^{(2)} = V_p^{CPTM} \sim \bar{n}_e \cdot const(r) \cdot F(p_e)/(r \cdot B_T \cdot n_e(r))$. First one is proportional to Ware pinch value, the second one is the particle pinch defined using the canonical profile transport model [9], where $F(p_e)$ is the deviation of electron pressure profile from the canonical one. Particle flux has been chosen to match the experimental behavior of line averaged density measured along the central chord. Typical distribution is presented in Fig. 3. Three shots have been chosen for the modeling: low density shot 33957 ($\bar{n}_e / n_{Gw} = 0.2$, $\nu_{eff} = 0.4$),

medium density shot 33965 ($\overline{n_e}/n_{Gw} = 0.5,\ \nu_{eff} = 2$) and high density shot 33970 ($\overline{n_e}/n_{Gw} = 1.1,\ \nu_{eff} = 9$). Results of the modeling are summarized in Fig. 4.

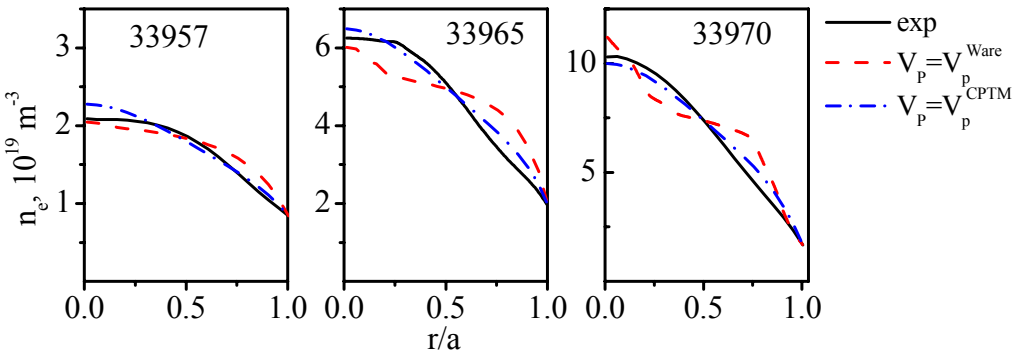

Fig. 4 Comparison between experimental and modeled density profiles.

It has been shown by modeling that according to the increase of $E_{||}$ the Ware pinch effect increases with the density (collisionality) increase. However, it can not describe well the density profile behavior which has been observed experimentally (Fig. 4). Particle pinch given by V_p^{CPTM} demonstrates much better agreement with the experiment. Therefore conclusion can be made that neoclassical pinch alone can not explain the density peaking with the density (collisionality) growth in T-10. Additional turbulent pinch should be considered.

Turbulent particle pinch is usually considered by modern theories as the result of the drift turbulence development. Two modes are usually discussed as the main players: Ion Temperature Gradient mode (ITG) and Trapped Electron Mode (TEM). Set of KINEZERO [10] calculations has been performed to estimate stability of drift turbulence in T-10 OH and ECRH heated plasmas. Results of calculations performed for L-mode case are shown in Figure 5. It is seen that the long scale modes are predicted to be unstable in a whole density range. Instability characterizes by $0.1<k_\theta\rho_i<1$ and rotates to the ion drift direction. The mode can be identified as ITG mode. Electron modes (rotating to the electron drift direction) TEM and ETG (Electron Temperature Gradient mode) instabilities, that characterizes by $k_\theta\rho_i\sim1$ and $k_\theta\rho_i\sim30$, are predicted to be stable at low and medium densities ($\overline{n}_e/n_{Gw} < 0.6$) and become unstable at high density ($\overline{n}_e/n_{Gw} \geq 0.85$). (Note that the similar behavior is predicted for OH discharges.) Thus KINEZERO calculations predict appearance of small scale (electron) instabilities with the density growth. This pattern is agrees qualitatively with the results of reflectometry measurements presented in [11]. However transport modeling shows that in L-mode the heat flux through the ion component is low in comparison with electron heat flux in a whole density range. Therefore it could be expected that in spite of the existence of ITG instability it does not play the crucial role in heat and particle transport in

T-10 L-mode. Since the T_e/T_i ratio is high in a whole density range: $T_e/T_i(r/a=0.5)\sim6.5$ at low density and ~1.5 at the highest one, therefore in a contrast to KINEZERO predictions and reflectometry measurements TEM could be expected as a more influential mode in a whole density range. In this case the density peaking with collisionality could be a complex effect of partial TEM stabilization (i.e. decrease of the outward particle flux usually linked to this mode at high T_e/T_i ratio) due to collisionality increase and increased influence of Ware pinch. The reasons of this possible contradiction are the subject for further analysis. Note here that in all discharges mentioned above the pressure peaking factor remains constant in a whole collisionality range.

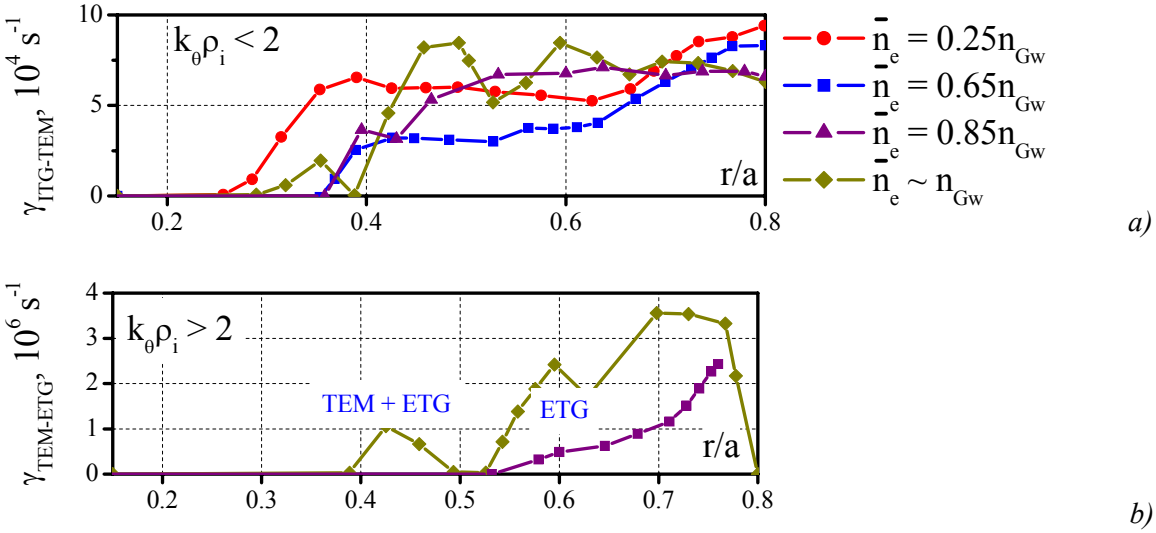

Fig. 5. Radial distribution of most unstable drift mode increment calculated by KINEZERO Code for long scale instabilities (a) and small scale instabilities (b).

This work has been supported by Nuclear Science and Technology Department of Rosatom and Scientific School Grant (Contract No. 02.516.11.6068)

[1] ITER Phys. Bas., Nucl.Fus. 39 (1999) 2137

[2] Weisen H. et al Nuclear Fusion 45 (2005) L1

[3] Garbet X. Plas. Phys. Contr. Fus. 46 (2004) B557

[4] Angioni C. et al Phys. Plas. 10 (2003) 3225

[5] Romanelly M. et al in Proc. Of 33rd EPS Conf. on Plasma Phys. Rome, 19 - 23 June 2006 ECA Vol.30I, P-5.074 (2006)

[6] Esipchuk Yu.V. et al Plasma Phys. Control. Fusion 45 (2003) 793

[7] Ware A.A.Phys. Rev. Let. 25 (1970) 15

[8] Pereverzev G. Preprint IAEA-5358/6, 1992

[9] Dnestrovskij Yu.N. et al. Plasma Phys. Reports, 23 (1997) 566

[10] Bourdelle C. Nucl.Fus. 45 (2005) 110

[11] Vershkov V. Nucl.Fus. 45 (2005) S203